

ELEMENTARY PARTICLES AND FIELDS

Experiment

Design of the Simulation Scheme for SPHERE-3 Telescope for the 10^{15} – 10^{18} eV Primary Cosmic Ray Studies Using Direct and Reflected Cherenkov Light from the Extensive Air Showers

E. A. Bonvech^{1)*}, C. J. Azra²⁾, D. V. Chernov¹⁾, V. I. Galkin^{1),2)}, E. L. Entina¹⁾,
V. A. Ivanov²⁾, V. S. Latypova¹⁾, D. A. Podgrudkov^{1),2)}, T. M. Roganova¹⁾, and M. D. Ziva^{1),3)}

Received August 1, 2023; revised August 1, 2023; accepted August 1, 2023

Abstract—Paper contains the first results on the development of a SPHERE-3 telescope for the primary cosmic ray studies in 1–1000 PeV energy range using reflected and direct Cherenkov light generated by extensive air showers. It also sheds some light on the development of our new approach to the design of the new telescope.

DOI: 10.1134/S1063778824010149

1. INTRODUCTION

In recent publications some indications appeared that a substantial part of the primary cosmic ray (PCR) in the 1 to 1000 PeV energy range might be of extragalactic origin [1]. Despite numerous attempts at partial spectra reconstructions they still have high uncertainties [2–4]. KASCADE-Grande experiment was able to reconstruct only two nuclei groups' spectra [5] due to uncertainty in high energy hadron–hadron interaction models. The results of various experiments on PCR mass composition using extensive air showers (EAS) data show poor agreement in the 3–50 PeV energy range [4–8]. PCR mass composition studies at 1–1000 PeV energy range might provide data that will help to refine models of cosmic ray acceleration and propagation in the Galaxy. But this problem of PCR mass composition above 1 PeV at present is far from solution. New measurements and experiments sensitive to the PCR mass composition are needed.

SPHERE-2 was one of such experiments and some data on the PCR mass composition was obtained using its measurements [9]. Now a new project of a new detector of the same type is under development, taking advantage of the important lessons learned during the design, operation and data analysis of the previous experiment.

In the long run the aim of the new project is to design the SPHERE-3 telescope, which, on one hand, will be aimed at obtaining the best possible estimates of EAS primary particle parameters, and, on the other hand, will result in a new knowledge on how to design other detectors of the type. Analysis of the Cherenkov light images' samples using developed processing codes allows to obtain the uncertainties of the EAS primary parameters, which, in turn, allow access to the expected measurements' quality with a given version of the telescope and the procedures for data processing. As a result, the optimal version of the telescope will be selected and a general approach to the choice of its design and data processing algorithms will be developed.

In addition to the previous experiment setups (SPHERE-1 and -2) the project aims to account for a possibility to detect both the reflected and direct Cherenkov light from the same EAS, which might help substantially to reduce the uncertainties of shower parameter reconstruction.

2. DIRECT CHERENKOV LIGHT IN SPHERE-2 DATA

During SPHERE-2 data analysis an unusual event was discovered where a normal Cherenkov image was positioned in an unusual location in the 'frame' preceded by what is an unintended direct Cherenkov light registration. Figure 1 shows both usual (*a*) and unusual (*b*) Cherenkov events.

In general case the trigger system selects the light flashed from EAS over the constant background of starlight snow (Fig. 1*a*). In the unusual event (Fig. 1*b*) the reflected Cherenkov light flash (easily

¹⁾Skobel'syn Institute of Nuclear Physics of Moscow State University, Moscow, Russia.

²⁾Faculty of Physics, Moscow State University, Moscow, Russia.

³⁾Faculty of Computational Mathematics and Cybernetics, Moscow State University, Moscow, Russia.

*E-mail: bonvech@yandex.ru

identifiable by a unique wave-like structure) was positioned in the frame 4 μs after the trigger, that occurred due to an extremely short light pulse (less than 50 ns) synchronous across different pixels. The detector at this moment was 603 m above the snow. The zenith angle of this shower was estimated as 17° . Light travel time there-and-back for 600 m is 4 μs that allows to conclude that both light flashes were of the same shower: first, EAS Cherenkov light directly illuminated pixels through the small slits between the mirror segments, second, the light traveled to the snow, was reflected and illuminated the detector the intended way. The slits in the mirror were unintended and were initially covered by cloth but under wind at working altitudes some slits became open.

The new telescope SPHERE-3 intentionally will make use of both reflected and direct Cherenkov light (CL). We are not decided yet on the way the direct CL is to be measured. First possibility is to make a hole in the center of the mirror which will be used as an aperture for the downgoing photons approaching the SiPMs of the mosaic. Thus, their angular distribution will be recorded before the reflected CL can reach the same sensors. The second option is to design a special detector for the direct CL, aimed at zenith and capable of analyzing its angular distribution. Probably, one can perceive some other ways of the direct CL detection or even their combinations. It is worth noting that at the moment all of them seem to be equally possible because 1) the design of the mirror is under way and 2) nothing will bar the view of such a detector as an unmanned aerial vehicle will be used as a carrier for SPHERE-3.

Angular distribution of EAS Cherenkov light is known to bear important information on the shower primary parameters, including the mass (type) of the primary particle. The most vivid example is the rapid advance of the imaging air Cherenkov telescopes for the gamma-ray astronomy studies [10, 11], that use EAS Cherenkov light angular distribution to distinguish gamma and nuclei induced showers. However, there is more information available, previously we have proposed a novel EAS study method by the construction of a new algorithm of processing the EAS Cherenkov light angular distribution aiming at estimating the mass of the primary nucleus [12, 13]. This makes us confident that the detection and proper processing of the EAS direct Cherenkov light angular image, alongside with the reflected one, will help to accurately estimate the primary mass. Therefore, we are going to design a new generation of SPHERE telescopes with a capability to simultaneously detect the reflected and direct Cherenkov light.

3. EAS CHERENKOV LIGHT SIMULATIONS

The design of a new SPHERE-3 telescope (or, hopefully, a series of them) will be based on vast and comprehensive simulations of the air cascades, of the process of Cherenkov light detection by the telescope, of the processes in electronic devices and, finally, of the data handling procedures.

First of all, the simulation of the EAS Cherenkov light images for both reflected and direct Cherenkov light are time consuming and require careful management.

Large number of Cherenkov photons even in 1 PeV EAS compelled us to refrain from the standard Cherenkov output file of the CORSIKA package [14]. The output was substituted by a binary file containing the Cherenkov photons' distributions at snow level and three flight altitudes packed in multidimensional arrays with suitable cell sizes: 2.5 m and 5 ns for snow surface and 10 m, 1° and 2 ns for higher altitudes. The convenience of such Cherenkov light characteristic representation lies in compactness and completeness: one archived EAS event amounts to about 500 MB and still contains rather detailed information on the shower so that it can be used many times. That is what we really do at stage 2 generating 100 clones of an event, which at stage 3 are converted into Cherenkov reflected or direct images. Clones only differ by the shower core location which is uniformly spread within a circle of 300–800 m radius (depending on the flight altitude) with the center at the telescope axis. We do not use the standard particle output file of CORSIKA as well, our modified code does not produce the file.

3.1. Reflected Cherenkov Light Simulations

The process of simulation of the images of reflected Cherenkov light in the SPHERE-2 telescope includes four stages (Fig. 2, upper right part):

1. Production of artificial EAS events with CORSIKA code, resulting in spatial-temporal distribution of Cherenkov photons on the snow surface; CORSIKA makes it possible to account for the properties of the particular PMTs used, namely, to track and record only the photons producing photoelectrons with unit probability, which save the simulation time. Several models of the Earth atmosphere and at least two models of hadron interaction (QGSJET01 [15–18] and QGSJETII-04 [19, 20]) standard for CORSIKA will be used.

2. Gathering of Cherenkov photons reflected from the snow surface on the aperture of the telescope taking into account the snow properties and the mutual geometry of the point of reflection and the detector position.

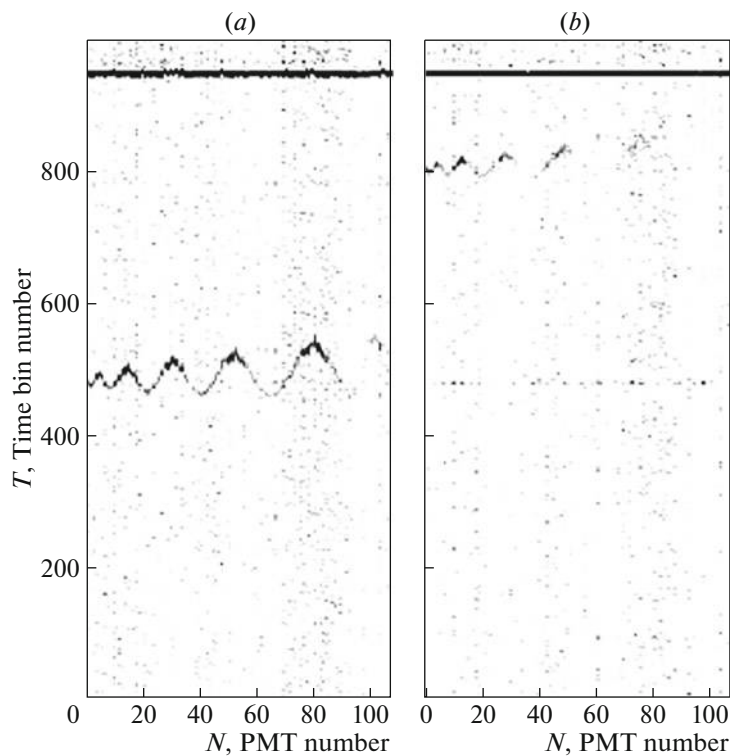


Fig. 1. Examples of Cherenkov light events detected in the SPHERE-2 experiment. (a) Regular reflected Cherenkov light event. (b) Event with direct and reflected Cherenkov light. Time bin width is equal to 12.5 ns.

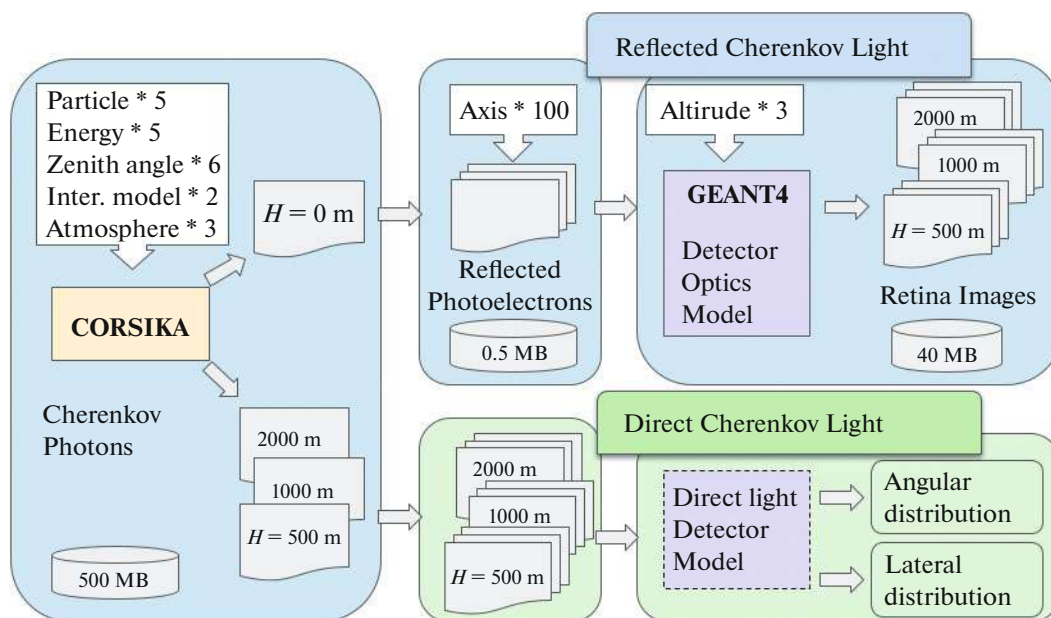


Fig. 2. Simulations pipeline.

3. Tracking the photons through the detector with Geant4 which involves absorption on the non-sensitive surfaces, reflection from the mirror and detection while a photon hits a mosaic of optical sensors of the telescope.

4. Conversion of the detected photons into electric

signals according to the model of the photosensors and the associated electronic devices (not to be described in this paper).

The general scheme of the SPHERE-3 design was described in [21]. A current version of the SPHERE-3 telescope optical part is shown

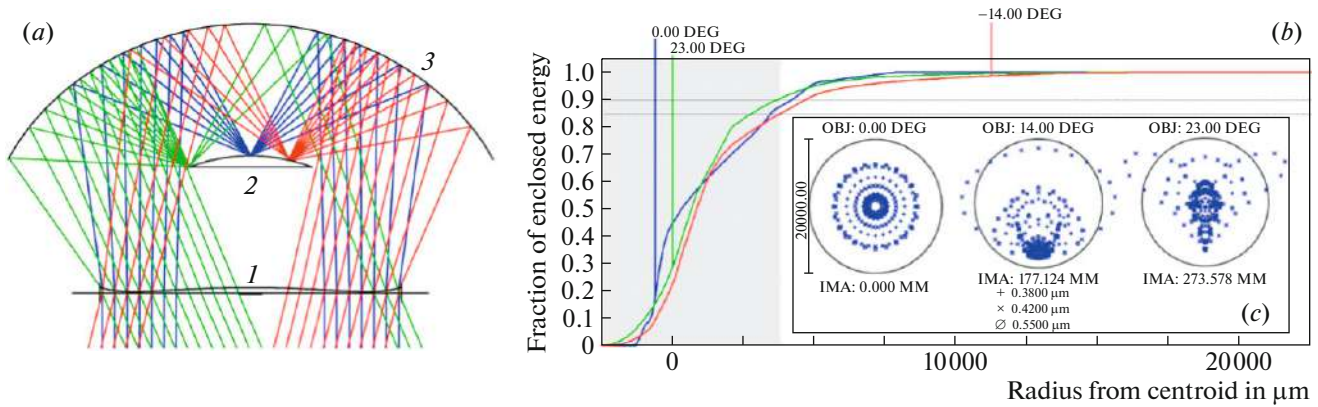


Fig. 3. Preliminary design of the optical part of the SPHERE-3 detector. (a) The layout of the optical components: 1—corrector lens, 2—photosensor mosaic, 3—aspherical mirror. (b) Fraction of energy contained within a spot of varying radius for different light bunch inclinations, and (c) spot diagrams at different angles for different wavelengths (300, 420 and 550 nm).

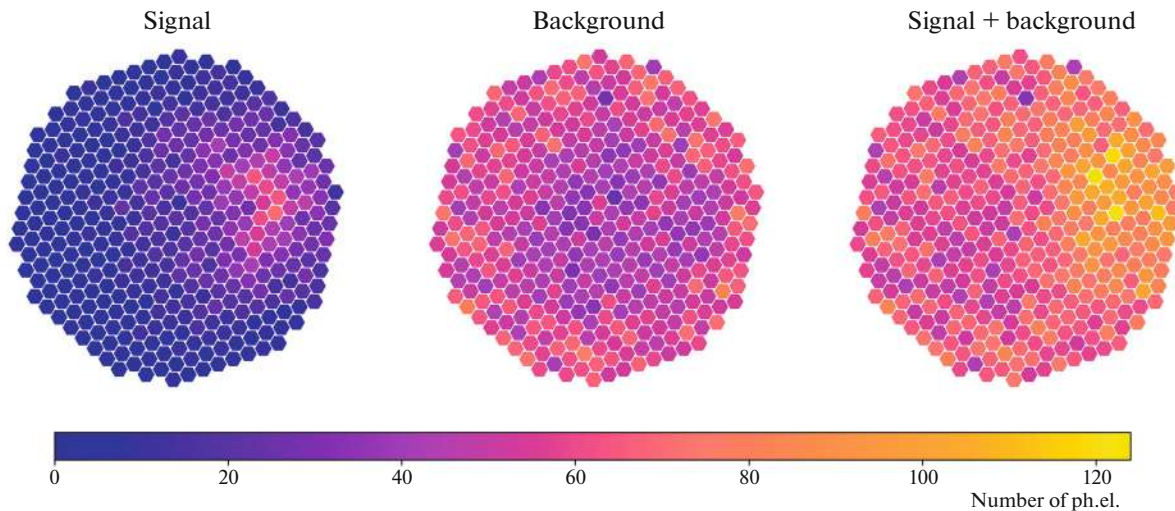


Fig. 4. Simulated images of the reflected Cherenkov light from EAS on the mosaic of SPHERE-3 telescope. Primary particle is a 10 PeV proton with 15° zenith angle, observation altitude 500 m above the snow level. Shower core is 89 m away from the telescope axis. The images show the light distribution over the mosaic segments, each segment incorporates 7 pixels.

in Fig. 3a. It includes a 2160 mm diameter aspherical mirror (3), a 1344 mm diameter aspherical corrector (1) and a 550 mm SiPM mosaic (2). The effective aperture of this design is 1.18 m^2 . The main light losses occur due to the shading of the mirror by the SiPM mosaic. For this version of the telescope the full viewing angle of the detector is 46° . It is assumed that the typical average diameter of one pixel with a $6 \times 6 \text{ mm}$ SiPM and a hexagonal lens light collector will be about 10 mm. Figure 3c shows the size of the light spot at different view angles: 0° , 14° , and 23° for different wavelengths (300, 420 and 550 nm). Figure 3b shows the graphs of the enclosed energy fractions vs. the spot radius show that within a 10 mm spot, depending on the inclination, 0.86 to 0.90 of the total flux is collected.

Figure 4 shows the results of the reflected Cheren-

kov light simulation for an EAS initiated by a primary proton of energy 10 PeV, zenith angle 15° , and core distance 89 m observed by a detector presented in Fig. 3 and at 500 m altitude above the snowed surface. The images were calculated for a mosaic consisting of 2653 SiPM. For the sake of clarity, the pixels were clustered in segments: 1 segment = 7 pixels. The night sky background was taken into account, it was assumed to be reflected from the snow at uniformly spread points and was then mixed with the signal.

3.2. Direct Cherenkov Light Calculations

In the case of the SPHERE-3 telescope another simulation sequence will be added to produce the images of direct EAS Cherenkov light. It incorporates similar four steps (Fig. 2, lower right part) as for the reflected Cherenkov light:

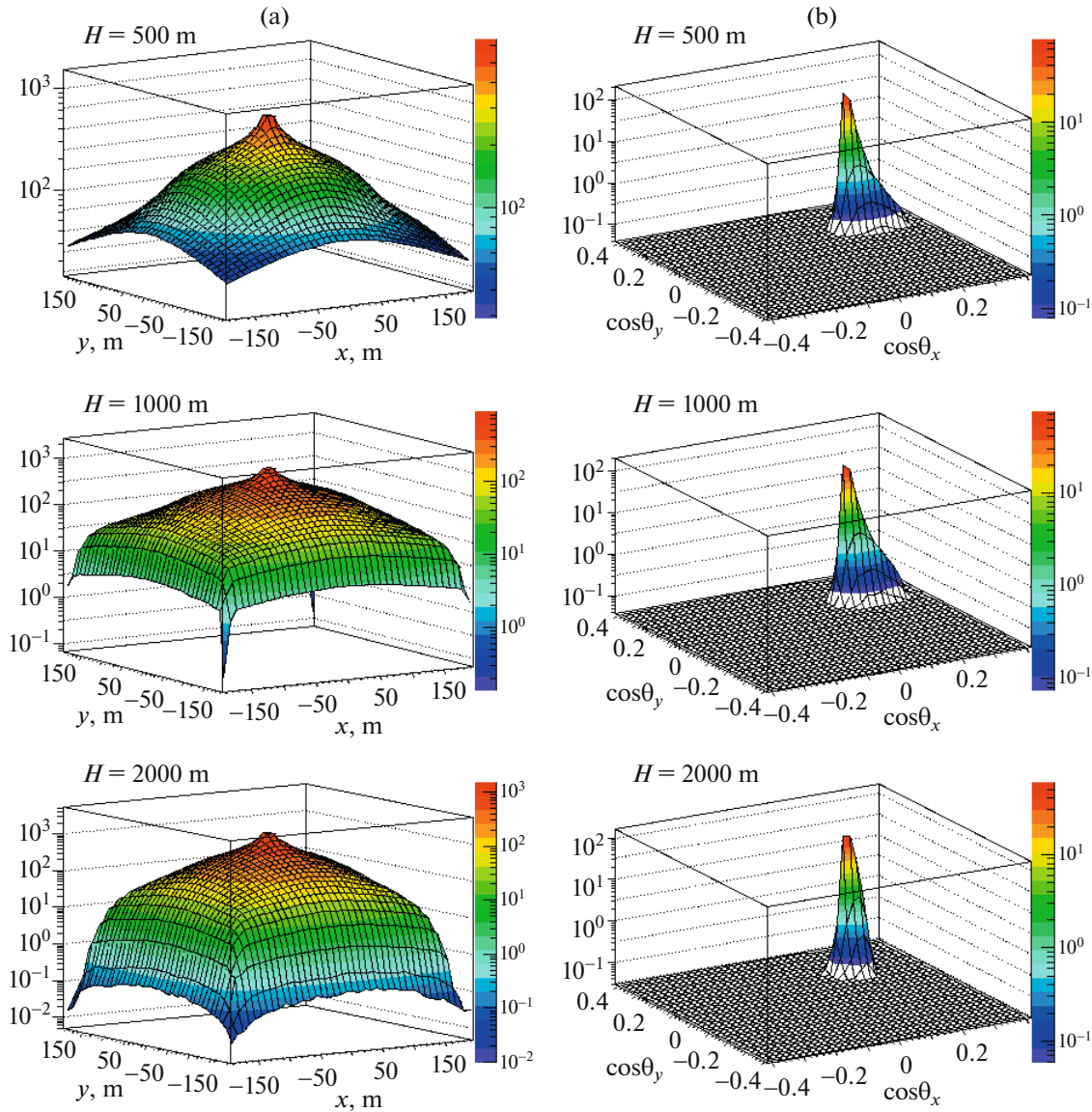


Fig. 5. (a) Spatial distribution of direct Cherenkov light. (b) Angular distribution of direct Cherenkov light. Both plots come from the same single shower initiated by a 1 PeV primary proton with zenith angle $\Theta = 15^\circ$. The spatial distribution is the total over the field of view ($50^\circ \times 50^\circ$), horizontal axes show detector position with respect to the shower core, vertical scale is in photoelectrons per 100 cm². The angular distribution (b) is shown for 105 m core distance, vertical scale is in photoelectrons per dm² per solid angle bin (which is $1^\circ \times 1^\circ$), horizontal axes show direction cosines of Cherenkov photons. Each plot is labeled with the flight altitudes.

1. Cherenkov photon distribution over space, time and direction is recorded by a slightly modified CORSIKA code at three different levels above the snow surface (500, 1000 and 2000 m) while simulating an EAS event.

2. Based on these distributions the Cherenkov photons entering the direct Cherenkov light part of the SPHERE-3 telescope (whatever it may be) are selected for tracing.

3. Tracing the photons through this part of the detector with Geant4. Direct Cherenkov light detector

is assumed to have a $50^\circ \times 50^\circ$ field of view and 1 dm² area.

4. Conversion of the detected photons into electric signals.

Figure 5 shows examples of lateral and angular distributions of direct Cherenkov light from an individual 15° zenith angle EAS initiated by an 1 PeV proton. A virtual detector of area 100 cm² and a field of view $50^\circ \times 50^\circ$ aims at zenith, angular bin is $1^\circ \times 1^\circ$, time bin is 2 ns. The data are recorded at three different levels: 500, 1000 and 2000 m above the snow level (as specified in the figures). One

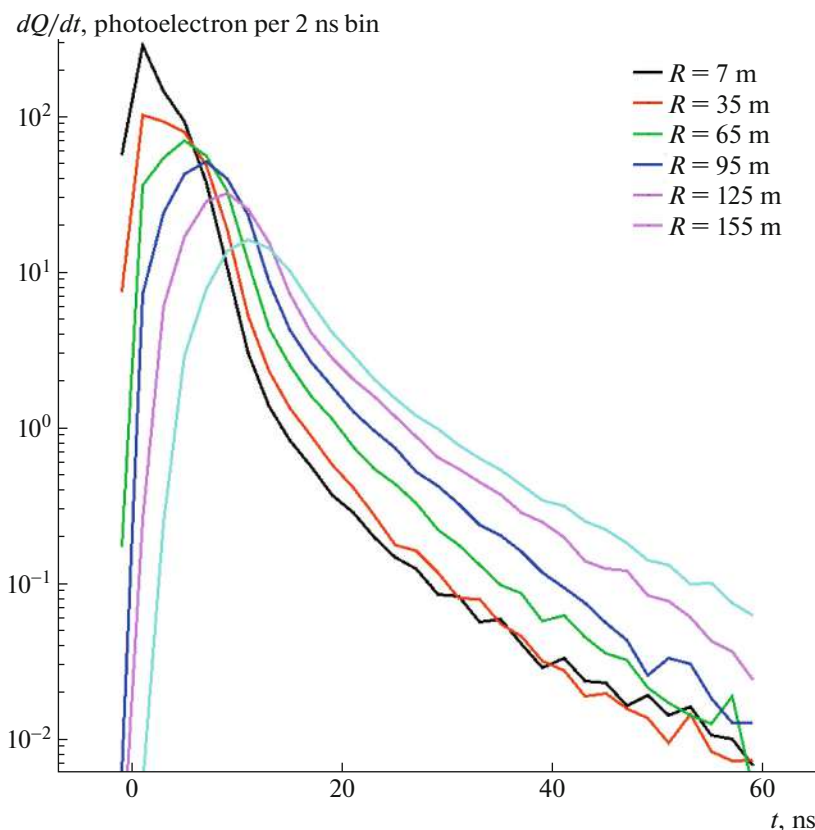


Fig. 6. Direct Cherenkov light pulses at the altitude $H = 500$ m above snow level for the same shower ($1 \text{ PeV} \Theta = 15^\circ$ primary proton) as shown in Fig. 3. The pulses are summed over the full field of view angle $50^\circ \times 50^\circ$, vertical scale is in photoelectrons per 100 cm^2 per time bin (2 ns).

can conclude from Fig. 5a that with a small-area detector it is only possible to use the direct Cherenkov light in ~ 100 m radius from the shower axis and this constraint becomes more stringent as the observation altitude increases. Figure 5b gives us the characteristic shapes of Cherenkov light angular distribution at different levels and justifies the choice of the angular bin size.

Figure 6 presents the Cherenkov light pulses at different core distances for the same proton EAS for 500 m above the snow. The pulse shape and magnitude allows reliable detection of the shower and accurate determination of arrival time of the Cherenkov light front.

Next step should be the analysis of Cherenkov light angular distributions from showers produced by different nuclei with a view of distinguishing between them. As of now our samples of artificial EAS with both direct and reflected CL calculated are too sparse to put forward any concrete technique. Still it is already clear that the direct CL angular distribution simple characteristic like the light spot long size provides a possible instrument to distinguish the showers according to the primary particle mass. Being combined with the selection parameters found for the

reflected CL [22] it (or some other features) is likely to boost the telescope's sensitivity toward the primary mass. We are going to give more details on the properties of the EAS images in the direct CL in the future papers.

4. STATUS OF THE PROJECT

The above shown descriptions of the simulation procedures, database structures and examples of the EAS Cherenkov light characteristics are just elements of our plan to design a new SPHERE telescope capable of accessing the PCR mass composition problem at high energies. The plan suggests considering a number of telescope designs and data analysis approaches from the viewpoint of their joint abilities to reconstruct the EAS primary parameters with focus on primary particle mass. The term 'telescope design' means not only the optical scheme but also the properties of sensors and dedicated electronics, the logic of data acquisition systems and, finally, each version of the telescope will be modeled to the level of their primary parameter uncertainties. All versions considered will be compared, which will allow us to choose the best design and data analysis

approach, and, secondly, will allow us to advance in the basic principles of the telescopes' design technique.

Presently the simulations are in progress and we are trying to find out how the direct Cherenkov light can help reduce the uncertainties of the EAS primary parameters.

5. CONCLUSIONS

In event with both the direct and reflected EAS Cherenkov light was found in the SPHERE-2 data. That was a starting point of the idea to use a combination of the direct and reflected Cherenkov light methods.

A preliminary version of the SPHERE-3 optical scheme is shown as a basis for further improvement and development of optimized optical schemes that will be combined with various schemes of sensitive mosaics, electronics, trigger algorithms and off-line processing algorithms.

The description of the created database of artificial events of EAS with the generation of Cherenkov light for protons, nitrogen and iron nuclei with energies in the range of 1–100 PeV and zenith angles of 5° – 25° according to two models of interaction and three models of the atmosphere is given.

A scheme for calculating artificial images of reflected and direct EAS Cherenkov light on the mosaic of optical sensors of the telescope is presented.

We also show the preliminary results of our attempts in analyzing direct EAS Cherenkov light.

FUNDING

The part of this work dedicated to the analysis of the SPHERE-2 experiment was supported by the Interdisciplinary Scientific and Educational School of Moscow University “Fundamental and Applied Space Research”.

The work was supported by the Russian Science Foundation no. 23-72-00006, <https://rscf.ru/project/23-72-00006/>.

The research is carried out using the equipment of the shared research facilities of HPC computing resources at Lomonosov Moscow State University [23].

CONFLICT OF INTEREST

The authors of this work declare that they have no conflicts of interest.

REFERENCES

1. S. Thoudam, J. P. Rachen, A. van Vliet, A. Achterberg, S. Buitink, H. Falcke, and J. R. Hörandel, *Astron. Astrophys.* **595**, A33 (2016).
2. F. G. Schröder, *PoS* **385**, 030 (2019).
3. A. Aab, P. Abreu, M. Aglietta, E. J. Ahn, I. Al Samarai, I. F. M. Albuquerque, I. Allekotte, P. Allison, A. Almela, J. Alvarez Castillo, J. Alvarez-Muñiz, M. Ambrosio, G. A. Anastasi, L. Anchordouqui, B. Andrada, and S. Andringa, *Phys. Lett. B* **762**, 288 (2016).
4. A. Glushkov and A. Sabourov, *JETP Lett.* **98**, 655 (2013).
5. W. D. Apel, J. C. Arteaga-Velázquez, K. Bekk, M. Bertaina, J. Blümer, H. Bozdog, I. M. Brancus, E. Cantoni, A. Chiavassa, F. Cossavella, K. Daumiller, V. de Souza, F. Di Pierro, P. Doll, R. Engel, J. Engler, et al., *Astropart. Phys.* **47**, 54 (2013).
6. T. Antoni, W. D. Apel, A. F. Badea, K. Bekk, A. Bercuci, J. Blümer, H. Bozdog, I. M. Brancus, A. Chilingarian, K. Daumiller, P. Doll, R. Engel, J. Engler, F. Feßler, H. J. Gils, R. Glasstetter, et al., *Astropart. Phys.* **24**, 1 (2005).
7. M. G. Aartsen, R. Abbasi, Y. Abdou, M. Ackermann, J. Adams, J. A. Aguilar, M. Ahlers, D. Altmann, J. Auffenberg, X. Bai, M. Baker, S. W. Barwick, V. Baum, R. Bay, J. J. Beatty, S. Bechet, et al., *Phys. Rev. D* **88**, 042004 (2013).
8. M. G. Aartsen, M. Ackermann, J. Adams, J. A. Aguilar, M. Ahlers, M. Ahrens, C. Alispach, K. Andeen, T. Anderson, I. Ansseau, G. Anton, C. Argüelles, J. Auffenberg, S. Axani, P. Backes, H. Bagherpour, et al., *PoS* **385**, 014 (2019).
9. R. A. Antonov, T. V. Aulova, E. A. Bonvech, V. I. Galkin, T. A. Dzhatdov, D. A. Podgrudkov, T. M. Roganova, and D. V. Chernov, *Phys. Part. Nucl.* **46**, 60 (2015).
10. T. C. Weekes, M. F. Cawley, D. J. Fegan, K. G. Gibbs, A. M. Hillas, P. W. Kowk, R. C. Lamb, D. A. Lewis, D. Macomb, N. A. Porter, P. T. Reynolds, and G. Vacanti, *Astrophys. J.* **342**, 379 (1989).
11. A. V. Plyasheshnikov, A. K. Konopelko, F. A. Aharonian, M. Hemberger, W. Hofmann, and H. J. Völk, *J. Phys. G* **24**, 653 (1998).
12. V. I. Galkin, A. S. Borisov, R. Bakhromzod, V. V. Bartaev, S. Latipova, and A. Muqumov, *EPJ Web Conf.* **145**, 15004 (2017).
13. V. I. Galkin, A. S. Borisov, R. Bakhromzod, V. V. Bartaev, S. Z. Latipova, and A. R. Muqumov, *Moscow Univ. Phys. Bull.* **73**, 179 (2018).
14. D. Heck, J. Knapp, J. N. Capdevielle, G. Schatz, and T. Thouw, Report FZKA No. 6019 (Karlsruhe, 1998).
15. N. N. Kalmykov and S. S. Ostapchenko, *Phys. At. Nucl.* **56**, 346 (1993).
16. N. N. Kalmykov, S. S. Ostapchenko, and A. I. Pavlov, *Bull. Russ. Acad. Sci.: Phys.* **58**, 1966 (1994).

17. N. N. Kalmykov, S. S. Ostapchenko, and A. I. Pavlov, Nucl. Phys. B **52**, 17 (1997).
18. S. S. Ostapchenko, private commun. (2001).
19. S. S. Ostapchenko, Phys. Rev. D **83**, 014018 (2011).
20. S. S. Ostapchenko, Phys. Rev. D **89**, 074009 (2014).
21. D. V. Chernov, C. Azra, E. A. Bonvech, V. I. Galkin, V. A. Ivanov, V. S. Latypova, D. A. Podgrudkov, and T. M. Roganova, Phys. At. Nucl. **85**, 641 (2022).
22. V. S. Latypova and V. I. Galkin, Uch. Zap. Fiz. Fak. MGU, m14513 (2023, in press).
23. V. Voevodin, A. Antonov, D. Nikitenko, P. Shvets, S. Sobolev, I. Sidorov, K. Stefanov, V. Voevodin, and S. Zhumatiy, Supercomp. Front. Innov. **6** (2), 4 (2019).

Publisher's Note. Pleiades Publishing remains neutral with regard to jurisdictional claims in published maps and institutional affiliations.